

Description of Additional Supplementary Files

File Name: Supplementary Movie 1

Description: FRAP of cingulin in WT cells.

File Name: Supplementary Movie 2

Description: FRAP of cingulin in γ -actin-KO cells.

File Name: Supplementary Movie 3

Description: FRAP of ZO-1 in WT cells.

File Name: Supplementary Movie 4

Description: FRAP of ZO-1 in γ -actin-KO cells.

File Name: Supplementary Movie 5

Description: FRAP of ZO-1 in γ -actin-KO cells treated with DMSO.

File Name: Supplementary Movie 6

Description: FRAP of ZO-1 in γ -actin-KO cells treated with blebbistatin.

Reporting Summary

Nature Portfolio wishes to improve the reproducibility of the work that we publish. This form provides structure for consistency and transparency in reporting. For further information on Nature Portfolio policies, see our [Editorial Policies](#) and the [Editorial Policy Checklist](#).

Statistics

For all statistical analyses, confirm that the following items are present in the figure legend, table legend, main text, or Methods section.

n/a	Confirmed
<input type="checkbox"/>	<input checked="" type="checkbox"/> The exact sample size (n) for each experimental group/condition, given as a discrete number and unit of measurement
<input type="checkbox"/>	<input checked="" type="checkbox"/> A statement on whether measurements were taken from distinct samples or whether the same sample was measured repeatedly
<input type="checkbox"/>	<input checked="" type="checkbox"/> The statistical test(s) used AND whether they are one- or two-sided <i>Only common tests should be described solely by name; describe more complex techniques in the Methods section.</i>
<input checked="" type="checkbox"/>	<input type="checkbox"/> A description of all covariates tested
<input type="checkbox"/>	<input checked="" type="checkbox"/> A description of any assumptions or corrections, such as tests of normality and adjustment for multiple comparisons
<input type="checkbox"/>	<input checked="" type="checkbox"/> A full description of the statistical parameters including central tendency (e.g. means) or other basic estimates (e.g. regression coefficient) AND variation (e.g. standard deviation) or associated estimates of uncertainty (e.g. confidence intervals)
<input checked="" type="checkbox"/>	<input type="checkbox"/> For null hypothesis testing, the test statistic (e.g. F , t , r) with confidence intervals, effect sizes, degrees of freedom and P value noted <i>Give P values as exact values whenever suitable.</i>
<input checked="" type="checkbox"/>	<input type="checkbox"/> For Bayesian analysis, information on the choice of priors and Markov chain Monte Carlo settings
<input checked="" type="checkbox"/>	<input type="checkbox"/> For hierarchical and complex designs, identification of the appropriate level for tests and full reporting of outcomes
<input checked="" type="checkbox"/>	<input type="checkbox"/> Estimates of effect sizes (e.g. Cohen's d , Pearson's r), indicating how they were calculated

Our web collection on [statistics for biologists](#) contains articles on many of the points above.

Software and code

Policy information about [availability of computer code](#)

Data collection	Not applicable
Data analysis	Not applicable

For manuscripts utilizing custom algorithms or software that are central to the research but not yet described in published literature, software must be made available to editors and reviewers. We strongly encourage code deposition in a community repository (e.g. GitHub). See the Nature Portfolio [guidelines for submitting code & software](#) for further information.

Data

Policy information about [availability of data](#)

All manuscripts must include a [data availability statement](#). This statement should provide the following information, where applicable:

- Accession codes, unique identifiers, or web links for publicly available datasets
- A description of any restrictions on data availability
- For clinical datasets or third party data, please ensure that the statement adheres to our [policy](#)

Source data are provided with this paper. The raw images from immunofluorescence experiments generated in this study have been deposited in the FigShare database under the accession code: <https://doi.org/10.6084/m9.figshare.28295240>.

Research involving human participants, their data, or biological material

Policy information about studies with [human participants or human data](#). See also policy information about [sex, gender \(identity/presentation\), and sexual orientation](#) and [race, ethnicity and racism](#).

Reporting on sex and gender Not applicable

Reporting on race, ethnicity, or other socially relevant groupings Not applicable

Population characteristics Not applicable

Recruitment Not applicable

Ethics oversight Not applicable

Note that full information on the approval of the study protocol must also be provided in the manuscript.

Field-specific reporting

Please select the one below that is the best fit for your research. If you are not sure, read the appropriate sections before making your selection.

☒ Life sciences ☐ Behavioural & social sciences ☐ Ecological, evolutionary & environmental sciences

For a reference copy of the document with all sections, see [nature.com/documents/nr-reporting-summary-flat.pdf](https://www.nature.com/documents/nr-reporting-summary-flat.pdf)

Life sciences study design

All studies must disclose on these points even when the disclosure is negative.

Sample size	No statistical method was used to predetermine the sample size. However, for the immunofluorescence (IF) experiments, we captured as many images as possible in each experiment. To ensure statistical confidence, we obtained a minimum of 5 biological replicates for each independent experiment, and we analyzed around 30 junctions per biological replicates. With the exception of a few specific experiments mentioned in the manuscript, we conducted each experiment 3 times independently and pooled the data from the three replicates for the final graphs. Specific quantification numbers are provided in the figure legend. Finally, although the IF results were provided only for 1 clone in the manuscript, we performed all these experiments in 3 different clonal cell lines which gave essentially similar results. This approach is in agreement with standard practices in the field, ensuring the reproducibility and robustness of our findings.
Data exclusions	We used the nested analysis from Graphpad Prism to identify the outliers. Any detected outliers (only few data points) were excluded from the statistical analysis.
Replication	All experiments were performed at least 3 times except in very few cases (specified into the manuscript). For each experiment, the number of biological replicates is indicated in the figure legend.
Randomization	This is not relevant to this study as we selected representative images for every experiments. We did not have any experiments where randomization would be pertinent.
Blinding	This is not relevant for our study as cited above.

Reporting for specific materials, systems and methods

We require information from authors about some types of materials, experimental systems and methods used in many studies. Here, indicate whether each material, system or method listed is relevant to your study. If you are not sure if a list item applies to your research, read the appropriate section before selecting a response.

Materials & experimental systems

n/a	Involved in the study
<input type="checkbox"/>	<input checked="" type="checkbox"/> Antibodies
<input type="checkbox"/>	<input checked="" type="checkbox"/> Eukaryotic cell lines
<input checked="" type="checkbox"/>	<input type="checkbox"/> Palaeontology and archaeology
<input checked="" type="checkbox"/>	<input type="checkbox"/> Animals and other organisms
<input checked="" type="checkbox"/>	<input type="checkbox"/> Clinical data
<input checked="" type="checkbox"/>	<input type="checkbox"/> Dual use research of concern
<input checked="" type="checkbox"/>	<input type="checkbox"/> Plants

Methods

n/a	Involved in the study
<input checked="" type="checkbox"/>	<input type="checkbox"/> ChIP-seq
<input checked="" type="checkbox"/>	<input type="checkbox"/> Flow cytometry
<input checked="" type="checkbox"/>	<input type="checkbox"/> MRI-based neuroimaging

Antibodies

Antibodies used

- Mouse IgG2b monoclonal anti-gamma-actin #2A368E2
- Mouse IgG1 monoclonal anti-beta-actin #4C259H12
- Rat polyclonal anti-PLEKHA6 #RtSZR127
- Guinea pig polyclonal anti-PLEKHA7 #GP2737
- Rabbit polyclonal anti-NM2A #909801
- Rabbit polyclonal anti-NM2B #909901
- Mouse monoclonal anti-pan-actin #mab1501
- FITC-phalloidin # P5282
- Mouse monoclonal anti-GFP #11814460001
- Mouse monoclonal anti-beta-tubulin #32-2600
- Rat monoclonal anti-ZO-1 #R40.76
- Mouse monoclonal anti-ZO-1 #33-9100
- Rabbit polyclonal anti-cingulin #C532
- Rabbit polyclonal anti-beta-catenin #C2206
- Rabbit polyclonal anti-E-cadherin #7870
- Mouse monoclonal anti-E-cadherin #BD610181
- Rabbit polyclonal anti-Claudin-1 #51-9000
- Mouse monoclonal anti-Claudin-2 #32-5600
- Rabbit polyclonal anti-Claudin-3 #34-1700
- Mouse monoclonal anti-Claudin-4 #32-9400
- Rabbit polyclonal anti-Claudin-7 #34-9100
- Rabbit polyclonal anti-Claudin-8 #40-0700Z
- Rabbit polyclonal anti-Claudin-10 #38-8400

Validation

- Validation 2A368E2 and 4C259H12: Dugina et al 2009, DOI: 10.1242/jcs.041970
- Validation RtSZR127 and GP2737: Sluysmans et al 2021, DOI: 10.1091/mbc.E21-07-0355
- Validation 909801 and 909901: Weissenbruch et al 2021, DOI: 10.7554/eLife.71888
- Validation mab1501: https://www.merckmillipore.com/CH/fr/product/Anti-Actin-Antibody-clone-C4,MM_NF-MAB1501
- Validation P5282: https://www.sigmaaldrich.com/CH/fr/product/sigma/p5282?srsltid=AfmBOopeNmsOY1FRyv9KDNRW70Ye8iO_JZJRNfMecl3OJl3LKM_xJsx
- Validation 11814460001: <https://www.citeab.com/antibodies/8906830-11814460001-anti-gfp>
- Validation 32-2600: <https://www.citeab.com/antibodies/2399654-32-2600-beta-tubulin-monoclonal-antibody-2-28-33>
- Validation R40.76: Itoh et al 1993, DOI: 10.1083/jcb.121.3.491
- Validation 33-9100: Spadaro et al 2017, DOI: 10.1016/j.cub.2017.11.014
- Validation C532: Cordenonsi et al 1999, DOI: 10.1083/jcb.147.7.1569; Rouaud et al 2023, DOI: 10.1083/jcb.202208065
- Validation C2206: <https://www.citeab.com/antibodies/1201469-c2206-anti-catenin-antibody-produced-in-rabbit>
- Validation 7870: https://www.scbt.com/fr/p/e-cadherin-antibody-h-108?srsltid=AfmBOoqsXPmlMMq1msOqCXiafCype_4QRvDQ9JjTt8lJtSrkkOW2NM-S
- Validation BD610181: https://www.bdbiosciences.com/en-ie/products/reagents/microscopy-imaging-reagents/immunofluorescence-reagents/purified-mouse-anti-e-cadherin.610181?tab=citations_references; Capaldo et al 2007, DOI:10.1091/mbc.E06-05-0471
- Validation 51-9000: Arnold et al 2024, DOI: 10.1111/exd.15084
- Validation 32-5600: Raju et al 2020, DOI: 10.1172/JCI138697
- Validation 24-1700, 32-9400 and 34-9100: Furuse et al 2022, DOI: 10.1247/csf.22068
- Validation 40-0700Z: Sassi et al 2020, DOI: 10.1681/ASN.2019080790
- Validation 38-8400: Prot-Bertoye et al 2021, DOI: 10.1152/ajprenal.00579.2020

Eukaryotic cell lines

Policy information about [cell lines and Sex and Gender in Research](#)

Cell line source(s)

MDCKII (Madin-Darby Canine Kidney type II, female, tet-off) cell lines were kindly provided by A. Fanning from the University of North Carolina.
EpH4 (mouse mammary epithelial, female) cell lines were kindly provided by E. Reichmann from the Hebrew University of Jerusalem: Fialka I et al 1996, DOI: 10.1083/jcb.132.6.1115.
mCCD (Mouse Cortical Collecting Duct) cell lines were kindly provided by E: Féraillé from the University of Geneva: Wang Y.B. et al 2014, DOI: 10.1681/ASN.2013040429.

Authentication

Cell lines were not authenticated.

Mycoplasma contamination

Cells were regularly tested for mycoplasma contamination and were negative for mycoplasma.

Commonly misidentified lines (See [ICLAC](#) register)

No commonly misidentified cell lines were used.

Plants

Seed stocks	Not applicable
Novel plant genotypes	Not applicable
Authentication	Not applicable

A feedback circuitry involving γ -actin, β -actin and NM2A controls tight junction and apical cortex mechanics

Corresponding Author: Professor Sandra Citi

This file contains all reviewer reports in order by version, followed by all author rebuttals in order by version.

Version 0:

Reviewer comments:

Reviewer #1

(Remarks to the Author)

In this study by Mauperin et al., the authors investigated the roles of beta-actin and gamma-actin isoforms in regulating the organization and function of tight junctions in epithelial cells. They found that knockdown of gamma-actin increased non-muscle myosin 2A (NM2A) expression, which in turn resulted in an upregulation of beta-actin expression. Knockdown of gamma-actin also increased tight junction membrane tortuosity and altered tight junction dynamics.

This is a carefully performed and rigorous study. The manuscript is very clearly written, and the data is convincing. The literature overview and discussion are comprehensive. Some of the findings contrast with earlier studies that have examined the effects of isoform-specific actin knockdown in another cell line but the authors carefully discuss these differences. Overall, I believe the findings will be of broad interest to cell biologists and will help better understand the roles of actin isoforms in epithelial cell biology.

Some minor changes needed to data presentation are listed below:

Comments:

- 1) Line 152 – “Upregulation of NM2A was rescued by exogenous expression of gamma-actin” – this is not shown in Fig S3D, instead it shows immunoblot analysis of the expression levels of NM2A upon depletion of gamma-actin.
- 2) Lines 153-156 – a description of the panels in figure S3 that correspond to the IB and IF analysis is incorrect.

Minor comments

- 1) In Line 150, it would be “the junctional” instead of “then junctional.”

Reviewer #2

(Remarks to the Author)

I co-reviewed this manuscript with one of the reviewers who provided the listed reports. This is part of the Nature Communications initiative to facilitate training in peer review and to provide appropriate recognition for Early Career Researchers who co-review manuscripts.

Reviewer #3

(Remarks to the Author)

The paper entitled “A feedback circuitry involving γ -actin, β -actin and nonmuscle myosin 2A controls membrane cortex mechanics in epithelial cells” by Maupérin et al. describes the effects of γ -actin knockout on β -actin and nonmuscle myosin 2A expression, shape of tight junctions, and tension of apical cortex using γ -actin knockout MDCK II cells. The paper provides an important insight into the function and regulation of individual actin isoforms. However, several points should be addressed to prove the claims by the authors.

Major points

The authors claim that the expression level of β -actin is upregulated in γ -actin via nonmuscle myosin 2A. However, the effect of RNA interference of nonmuscle myosin 2A on β -actin expression is examined only in MDCK II cells. Since the expression level of nonmuscle myosin 2A is not affected by the β -actin depletion in SKCO 15 cells (Baranwal et al., 2012), it is required to demonstrate that nonmuscle myosin 2A is involved in the regulation of β -actin expression in other cell lines such as EpH4 and mCCD cells.

The tortuosity of tight junctions is increased in γ -actin knockout MDCK cells. Since RNA interference of β -actin results in the increase of nonmuscle myosin 2A expression but has no effects on the tortuosity in MDCK cells, the authors claim that both β -actin and nonmuscle myosin 2A are required for the regulation of tortuosity of tight junctions. It is unclear which isoform(s) of actin and myosin are important for the regulation of the tortuosity of tight junctions. It is required to examine the effects of the overexpression of actin and myosin isoforms on the tortuosity of tight junctions. In addition, various other factors including Shroom3, Willin/FRMD6, Lulu, Tuba and ZO-1 are involved in the regulation of the shape of tight junctions, and ROCK is involved in the mechanism of the regulation in some cases (Hildebrand, 2005; Ishiuchi et al., 2011; Nakajima and Tanoue, 2010). The authors should examine the effects of γ -actin knockout on these factors to elucidate the mechanism of the regulation of tight junction tortuosity. Also, the alignment of myosin and the ultrastructure of cytoskeleton are reported to correlate to the shape of tight junctions (Fanning et al., 2012). More detailed analysis of the structure of cytoskeleton in γ -actin knockout cells would be helpful to understand the mechanism of the regulation of tight junction tortuosity.

The authors claim that the rescue of γ -actin reverted the expression of β -actin. The expression level of γ -actin in the rescue experiment is surprising low (Fig. S2). In contrast, the authors also claim that the expression of β -actin is also increased by the RNA interference of γ -actin similar to the knockout of γ -actin (Fig. S2). However, the expression level of γ -actin seems to be much higher in knockdown cells than rescue cells. The authors should explain the reason of these results.

Minor points

In the leaky epithelia like MDCK II cells, charge selectivity is generally more sensitive to evaluate the barrier function of tight junctions. The measurement of charge selectivity (dilution potential) would be helpful for the evaluation of γ -actin knockout on the barrier function of tight junction (Fig. 4).

The terms "CGN" and "cingulin" are used in the manuscript and it is confusing. Please unify the term.

The authors discuss that the deafness by the overexpression of ZO-2 or knockout cingulin is related to the regulation of actin filament by ZO-2 or cingulin (lines 312-316). However, the barrier function of tight junction is known to be important to maintain the unique electrophysiological environment in the inner ear, which is required for the maintenance of hair cells. The authors should mention the possibility that the effect of ZO-2 or cingulin modification on the barrier function of tight junctions and electrophysiological environment in the inner ear.

Version 1:

Reviewer comments:

Reviewer #3

(Remarks to the Author)

I think my concerns have been addressed in the revised manuscript.

Open Access This Peer Review File is licensed under a Creative Commons Attribution 4.0 International License, which permits use, sharing, adaptation, distribution and reproduction in any medium or format, as long as you give appropriate credit to the original author(s) and the source, provide a link to the Creative Commons license, and indicate if changes were made.

In cases where reviewers are anonymous, credit should be given to 'Anonymous Referee' and the source.

The images or other third party material in this Peer Review File are included in the article's Creative Commons license, unless indicated otherwise in a credit line to the material. If material is not included in the article's Creative Commons license and your intended use is not permitted by statutory regulation or exceeds the permitted use, you will need to obtain permission directly from the copyright holder.

To view a copy of this license, visit <https://creativecommons.org/licenses/by/4.0/>

Reviewer #1 (Remarks to the Author):

In this study by Mauperin et al., the authors investigated the roles of beta-actin and gamma-actin isoforms in regulating the organization and function of tight junctions in epithelial cells. They found that knockdown of gamma-actin increased non-muscle myosin 2A (NM2A) expression, which in turn resulted in an upregulation of beta-actin expression. Knockdown of gamma-actin also increased tight junction membrane tortuosity and altered tight junction dynamics.

This is a carefully performed and rigorous study. The manuscript is very clearly written, and the data is convincing. The literature overview and discussion are comprehensive. Some of the findings contrast with earlier studies that have examined the effects of isoform-specific actin knockdown in another cell line but the authors carefully discuss these differences. Overall, I believe the findings will be of broad interest to cell biologists and will help better understand the roles of actin isoforms in epithelial cell biology.

Some minor changes needed to data presentation are listed below:

Comments:

- 1) Line 152 – “Upregulation of NM2A was rescued by exogenous expression of gamma-actin” – this is not shown in Fig S3D, instead it shows immunoblot analysis of the expression levels of NM2A upon depletion of gamma-actin.
- 2) Lines 153-156 – a description of the panels in figure S3 that correspond to the IB and IF analysis is incorrect.

Response. Thank you for pointing out these errors. The text was revised: “Moreover, up-regulation of NM2A was observed upon depletion of γ -actin by siRNA both in MDCK cells and in additional epithelial cell lines (mCCD and Eph4), as determined by IB analysis (Fig. S3D, quantification in Fig. S3E) and by IF analysis (Fig. S3F-H, quantifications on the right).”

Minor comments

- 1) In Line 150, it would be “the junctional” instead of “then junctional.”

Response. Thank you for detecting the typo. The text was revised.

Reviewer #2 (Remarks to the Author):

I co-reviewed this manuscript with one of the reviewers who provided the listed reports. This is part of the Nature Communications initiative to facilitate training in peer review

and to provide appropriate recognition for Early Career Researchers who co-review manuscripts.

Reviewer #3 (Remarks to the Author)

The paper entitled “A feedback circuitry involving γ -actin, β -actin and nonmuscle myosin 2A controls membrane cortex mechanics in epithelial cells” by Maupérin et al. describes the effects of γ -actin knockout on β -actin and nonmuscle myosin 2A expression, shape of tight junctions, and tension of apical cortex using γ -actin knockout MDCK II cells. The paper provides an important insight into the function and regulation of individual actin isoforms. However, several points should be addressed to prove the claims by the authors.

Major points

The authors claim that the expression level of β -actin is upregulated in γ -actin via nonmuscle myosin 2A. However, the effect of RNA interference of nonmuscle myosin 2A on β -actin expression is examined only in MDCK II cells. Since the expression level of nonmuscle myosin 2A is not affected by the β -actin depletion in SKCO 15 cells (Baranwal et al., 2012), it is required to demonstrate that nonmuscle myosin 2A is involved in the regulation of β -actin expression in other cell lines such as Eph4 and mCCD cells.

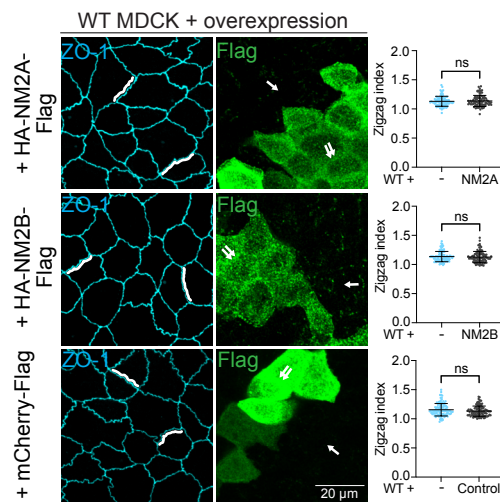
Response. We thank this Reviewer for suggesting this experiment. The same results were obtained with additional cell lines (Eph4 and mCCD) and are now shown in revised Fig. S3 (panels K-L).

The tortuosity of tight junctions is increased in γ -actin knockout MDCK cells. Since RNA interference of β -actin results in the increase of nonmuscle myosin 2A expression but has no effects on the tortuosity in MDCK cells, the authors claim that both β -actin and nonmuscle myosin 2A are required for the regulation of tortuosity of tight junctions.

Response. The text of Discussion was revised to include “The observation that increased NM2A expression in β -actin-depleted cells did not result in increased tortuosity suggests that γ -actin cannot functionally replace β -actin with regards to the generation and transmission of force from the circumferential belt to the TJ membrane.”

It is unclear which isoform(s) of actin and myosin are important for the regulation of the tortuosity of tight junctions. It is required to examine the effects of the overexpression of actin and myosin isoforms on the tortuosity of tight junctions.

Response. We carried out overexpression of NM2A and NM2B, and of either γ -actin or β -actin, and examined the effect of this overexpression on TJ membrane tortuosity. In the case of either NM2A or NM2B, we used FLAG-tagged versions, that were correctly delivered to junctions, as well as to the cortex and cytoplasm of cells (new experiment, shown in Reviewer Fig. 1).

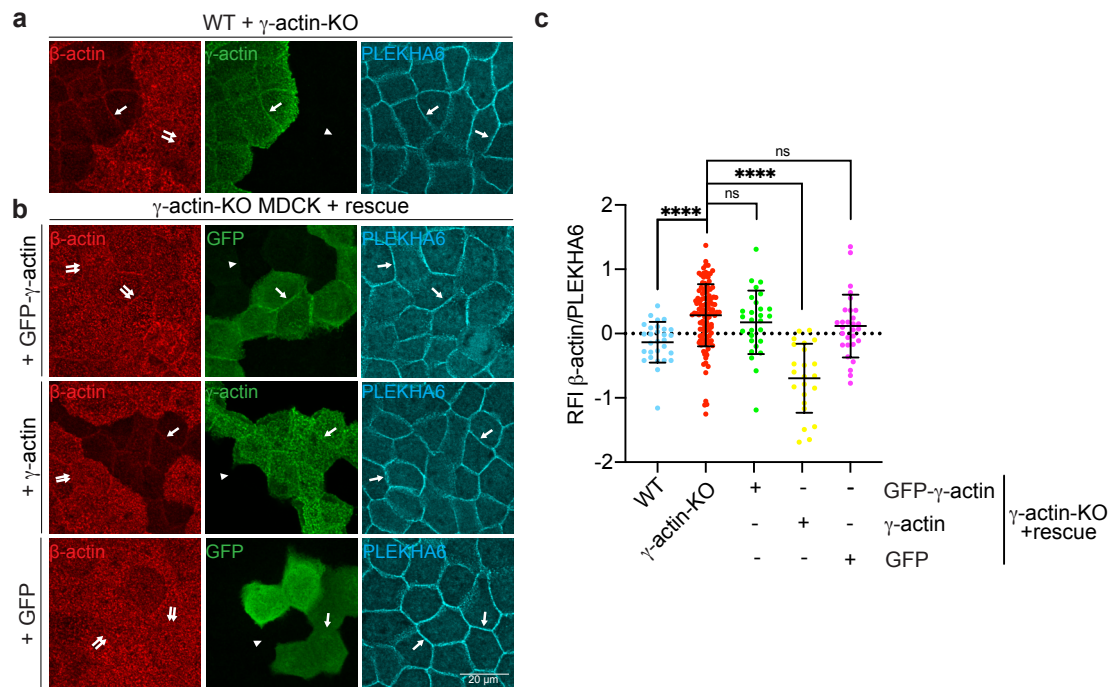


Reviewer figure 1_ NM2A and NM2B overexpression in WT MDCK cells doesn't affect the TJ-membrane tortuosity.

Immunofluorescence (IF) microscopy analysis and zig-zag index quantifications (on the right on IF panels) of endogenous ZO-1 (cyan), used as a TJ marker, in WT MDCK cells overexpressing full-length canis NM2A tagged with HA and Flag (HA-NM2A-Flag) (top panels), full-length canis NM2B tagged with HA and Flag (HA-NM2B-Flag) (middle panels) or by mCherry-Flag alone as negative control (bottom panels); distinguished via Flag antibody (green). Arrows indicate WT expression of NM2A and NM2B, double-arrows indicate overexpression of NM2A, NM2B or Control. The white line represents the TJ membrane tortuosity. Scale bar = 20 μ m. Dots shows replicates (N=3, n=97-110) and bars represent mean \pm SD. Statistical significance of quantitative data was determined by an unpaired Mann-Whitney's test (ns: not significant, ****p<0.0001).

However, no effect on TJ membrane tortuosity was observed. This can be explained by the likely possibility that NM2 filaments/monomers/oligomers at steady state are already functionally saturating the system. It is also possible that no more myosin filaments/molecules can be integrated beyond a homeostatic level in a WT context, where no cytoplasmic actin isoform has been depleted.

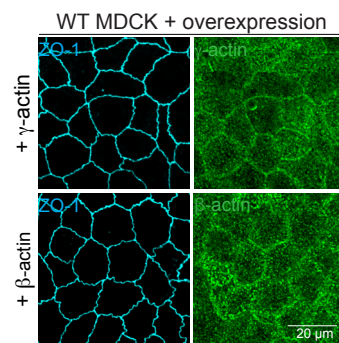
In the case of cytoplasmic actins, we found that GFP-tagged γ -actin is not functional, although it is targeted to junctions, because it does not rescue the phenotype of increased β -actin expression in γ -actin-KO cells (new experiment, shown in Reviewer Fig. 2). This is in agreement with previous studies on cytoplasmic actins, showing that tags interfere with actin function (Rommelaere et al 2004, doi: 10.1251/bpo94, Deibler et al 2011, <https://doi.org/10.1371/journal.pone.0022941>; Nagasaki et al 2017, <https://doi.org/10.1247/csf.17016>).



Reviewer figure 2_GFP-tagged γ -actin does not rescue the phenotype of increased β -actin localization in γ -actin-KO, unlike untagged γ -actin.

(a-c) Immunofluorescence (IF) microscopy analysis (a, b) and relative fluorescence intensity (RFI) quantifications (c) of endogenous β -actin (red) at junctions in mixed cultures of WT and γ -actin-KO (a); or in γ -actin-KO cells rescued with full-length canis GFP-tagged γ -actin (GFP- γ -actin) (top panels), full-length canis untagged γ -actin (γ -actin) (middle panel), or by GFP alone as negative control (bottom panels) (b). Arrows indicate normal labelling (as in WT cells), double-arrows indicate increased labelling for β -actin, arrowheads indicate loss of γ -actin labelling in KO cells. Quantification of RFI corresponds to the ratio between the junctional staining of β -actin versus the junctional marker PLEKHA6 (cyan). Scale bar = 20 μ m. Dots shows replicates and bars represent mean \pm SD. Statistical significance of quantitative data was determined by an unpaired Mann-Whitney's test (ns: not significant, **** p <0.0001).

When we used un-tagged forms of either γ -actin or β -actin, we could not distinguish WT from overexpressing cells (new experiment, shown in Reviewer Fig. 3), suggesting a rheostat mechanism that prevents expressing total levels of cytoplasmic actins beyond homeostatic levels (a mechanism that is similar to what described for “auto-regulation of tubulin expression, and for actin was described in the 80s and 90s by the Bershadsky and Be Ze’ev laboratories, but has not been studied further).



Reviewer figure 3_The cells overexpressing γ -actin or β -actin cannot be distinguished from the WT cells.

Immunofluorescence (IF) microscopy analysis of endogenous ZO-1 (cyan) at junctions in WT MDCK cells overexpressing full-length canis untagged γ -actin (γ -actin) (top panels) or full-length canis untagged β -actin (β -actin) (bottom panels) (green). Scale bar = 20 μ m. N=3.

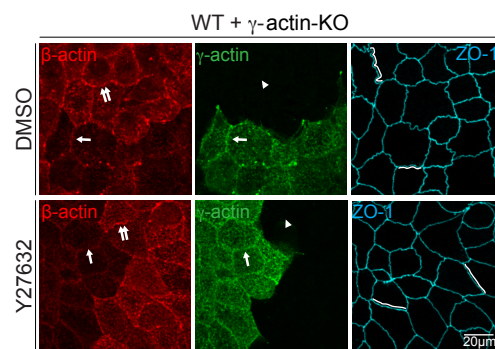
These results confirm our longstanding experience that overexpression experiments are often either technically problematic and prone to artifacts, or/and difficult to interpret, due to the saturation of the molecular systems by the endogenous proteins and/or to constraints due to spatial architecture, existing interactors etc. In contrast, depletion, KO and rescue experiments of specific cellular components provide much clearer and more interpretable phenotypes and results. We prefer to omit Reviewer Figures 1, 2, 3 from the paper, since they provide no additional useful information.

Comment:

In addition, various other factors including Shroom3, Willin/FRMD6, Lulu, Tuba and ZO-1 are involved in the regulation of the shape of tight junctions, and ROCK is involved in the mechanism of the regulation in some cases (Hildebrand, 2005; Ishiuchi et al., 2011; Nakajima and Tanoue, 2010). The authors should examine the effects of γ -actin knockout on these factors to elucidate the mechanism of the regulation of tight junction tortuosity.

Response. We performed a new experiment (Reviewer Fig. 4), and showed that treating mixed WT and γ -actin-KO cells with Y27632 (which inhibits the Rho-ROCK-dependent NM2 activation) results in decreased TJ membrane tortuosity. This is consistent with the known mechanistic implication of NM2 in TJ tortuosity in WT cells (Van Itallie et al 2009 doi 10.1091/mbc.E09-04-0320, Lu et al 2021 /doi.org/10.1101/2021.05.30.446323). We prefer not to include this Figure in the revised manuscript, since it is redundant with published evidence (Van Itallie et al 2009, etc).

Regarding the potential implication of all of the additional proteins cited by the Reviewer in the phenotypes of γ -actin-KO cells, our manuscript addresses the role of γ -actin and we demonstrate a mechanistic implication of NM2A. Addressing this question would require to open new lines of investigation and goes beyond the scope of this paper. The text of the discussion was revised to as follows: “TJ membrane tortuosity is the result of orthogonal forces generated by the contractility of the circumferential actomyosin bundle associated with apical junctions (Tang, 2018, Citi, 2019, Citi, 2024). As such, it is regulated by different proteins directly or indirectly associated with the actomyosin cytoskeleton, including ZO-1 (Van Itallie et al, 2009; Tokuda, 2014,), Shroom (Hildebrand, 2005), Lulu (Nakajima, 2011), cingulin (Rouaud, 2023) and other factors (reviewed in (Lynn, 2020)).



Reviewer figure 4 ROCK inhibition by Y27632 treatment decreases the TJ-membrane tortuosity in both WT and γ -actin-KO cells.

IF microscopy analysis of endogenous ZO-1 (cyan), used as a TJ marker, in mixed culture of WT and γ -actin-KO cells treated with DMSO (top panel) and Y27632 (bottom panel); distinguished via γ -actin (green). Arrows indicate normal labelling (as in WT cells), double-arrows indicate increased labelling for β -actin, arrowheads indicate loss of γ -actin labelling in KO cells. The white line represents the TJ membrane tortuosity. Scale bar = 20 μ m. N=3.

Also, the alignment of myosin and the ultrastructure of cytoskeleton are reported to correlate to the shape of tight junctions (Fanning et al., 2012). More detailed analysis of the structure of cytoskeleton in γ -actin knockout cells would be helpful to understand the mechanism of the regulation of tight junction tortuosity.

Response. *We carried out new experiments, and we now provide high resolution (STED) imaging, showing distinct pattern of the actin cytoskeleton, e.g. more intensely labeled contractile foci in the apical cortex of WT cells versus γ -actin-KO cells (new panel, Fig. 3F). The text of Results was modified accordingly.*

The authors claim that the rescue of γ -actin reverted the expression of β -actin. The expression level of γ -actin in the rescue experiment is surprising low (Fig. S2).

Response. *The levels are low because in this transient expression experiment only a small percentage of the cells are expressing the transgene. Fluorescent signals for actin in expressing cells are comparable to normal. The text was revised : “To confirm the specificity of the phenotype, we first rescued γ -actin-KO cells by re-expression of γ -actin, which was detected in transfected cells by IF at levels similar to WT (Fig. S2D, compare to Fig. 1A), though total protein levels were low, due to the low efficiency of transfection (IB analysis in Fig. S2E).”*

In contrast, the authors also claim that the expression of β -actin is also increased by the RNA interference of γ -actin similar to the knockout of γ -actin (Fig. S2). However, the expression level of γ -actin seems to be much higher in knockdown cells than rescue cells. The authors should explain the reason of these results.

Response. *As stated above, IB analysis shows total levels in depleted/undepleted and transfected/untransfected cells, while immunofluorescence analysis allows to detect specifically the levels of γ -actin and β -actin in depleted and rescue cells (Fig. S2 D, I-K), providing unambiguous evidence.*

Minor points

In the leaky epithelia like MDCK II cells, charge selectivity is generally more sensitive to evaluate the barrier function of tight junctions. The measurement of charge selectivity (dilution potential) would be helpful for the evaluation of γ -actin knockout on the barrier function of tight junction (Fig. 4).

Response. *Since the overall impact of the KO of γ -actin on both pore and leak pathway was not significant, and we observed no effect of γ -actin KO on the localization and junctional accumulation of TJ and AJ markers, we think there is no functional or molecular evidence supporting the need for a more detailed analysis of TJ barrier function.*

The terms “CGN” and “cingulin” are used in the manuscript and it is confusing. Please unify the term.

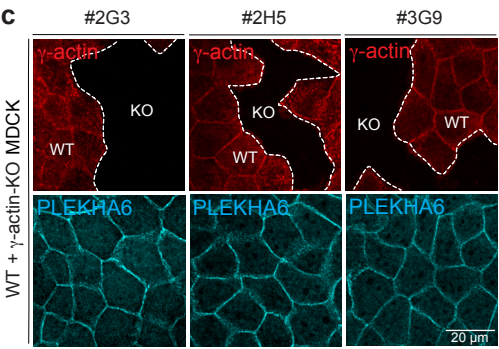
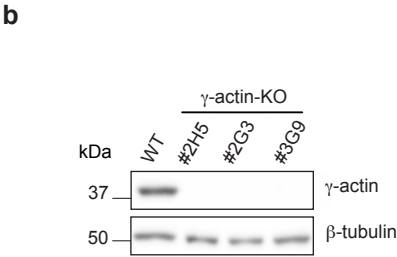
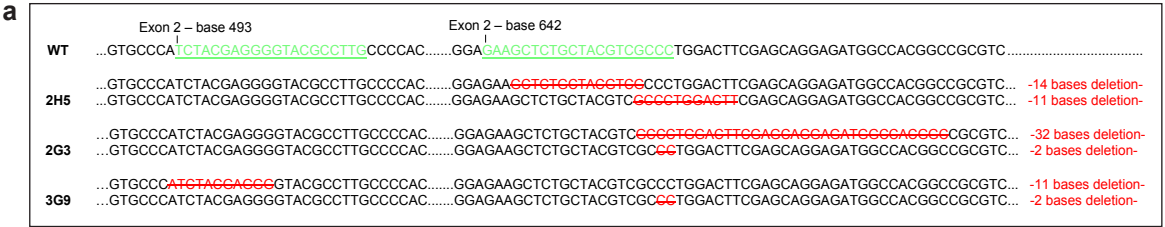
Response. We revised the manuscript and used cingulin consistently.

The authors discuss that the deafness by the overexpression of ZO-2 or knockout cingulin is related to the regulation of actin filament by ZO-2 or cingulin (lines 312-316). However, the barrier function of tight junction is known to be important to maintain the unique electrophysiological environment in the inner ear, which is required for the maintenance of hair cells. The authors should mention the possibility that the effect of ZO-2 or cingulin modification on the barrier function of tight junctions and electrophysiological environment in the inner ear.

Response. To address this point, the text of the Discussion was revised to include the additional mechanisms cited by this Reviewer, as follows: “Intriguingly, either KO or mutation of cingulin in mice and humans is associated with progressive hearing loss, through increased death and apoptosis of hair cells (Zhu, Huang et al. 2023). Our results suggest that cingulin and γ -actin control survival of hair cells and hearing function by maintaining apical membrane stiffness and cellular integrity upon mechanical stress, through their ability to anchor γ -actin and NM2B to TJs (cingulin) and provide the cortex with specific biophysical stiffness properties (γ -actin). Other mechanisms have been described through which TJ proteins can affect hearing, such as increased apoptosis induced by overexpression of ZO-2 (Walsh, Pierce et al. 2010) and altered TJ-dependent ionic permeability resulting from loss or mutations of claudins (Ben-Yosef, Belyantseva et al. 2003, Gow, Davies et al. 2004, Nayak, Lee et al. 2013), tricellulin (Nayak, Lee et al. 2013), and occludin (Kitajiri, Katsuno et al. 2014). However, such a mechanism is unlikely for cingulin and γ -actin, since there is insufficient evidence for a significant effect of their KO on barrier function of epithelial cells (Guillemot, Hammar et al. 2004, Guillemot, Schneider et al. 2012, Mauperin, Sassi et al. 2023).”

SUPPLEMENTARY INFORMATION

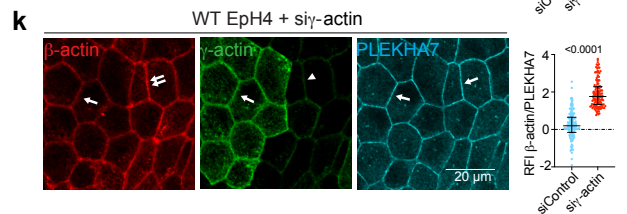
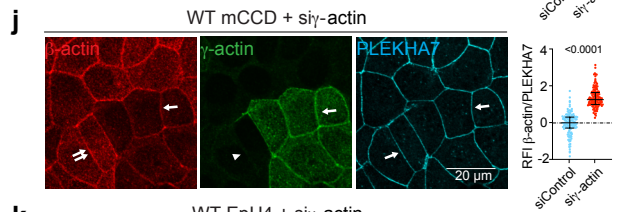
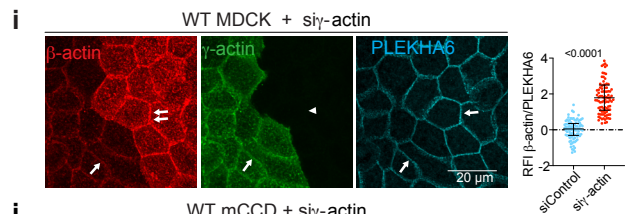
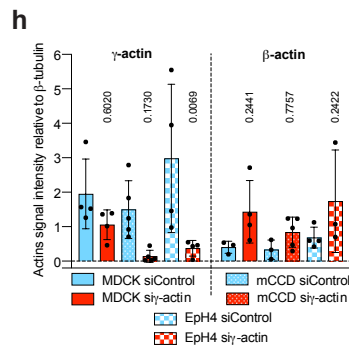
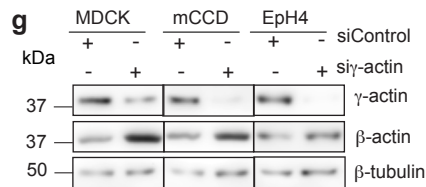
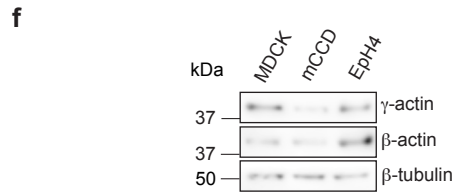
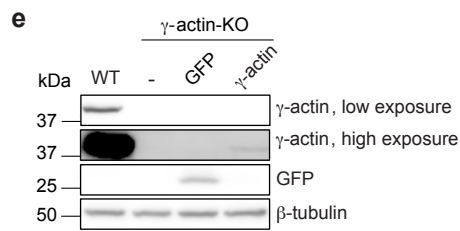
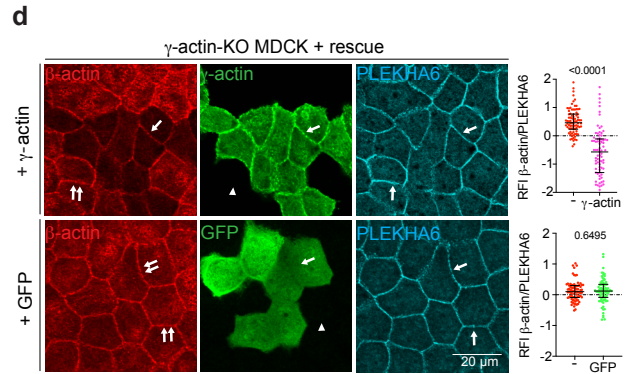
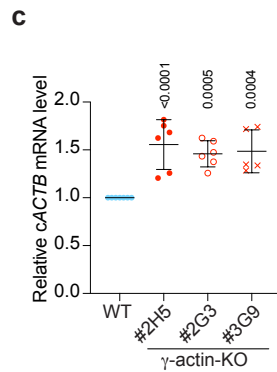
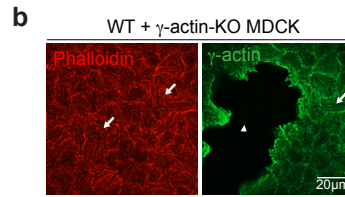
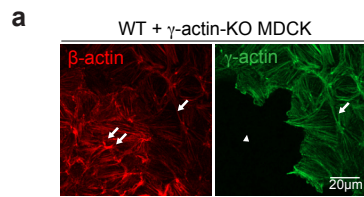
Supplementary Figures



Supplementary Figure 1. Generation of MDCK cells KO for γ -actin using Crispr/Cas9.

(a-c) Validation of Crispr/Cas9-mediated deletion of γ -actin in WT MDCK background by genomic sequencing (a), IB (b) and IF microscopy (c) analysis.

For genomic sequencing, Crispr targets are coloured in green in WT sequence with their position in the exon, base deletions in the alleles of the KO clones obtained are highlighted by strikeout red. For IB analysis, β -tubulin is used as a loading control. For IF microscopy analysis, PLEKHA6 is used as junctional marker reference. Scale bar = 20 μ m.



Supplementary Figure 2. The KO of γ -actin specifically affects the mRNA and protein expression of β -actin in different epithelial cell types.

(a-b) IF microscopy analysis of the localization of either β -actin (a) or phalloidin (b) in the basal region of mixed cultures of WT and γ -actin-KO MDCK.

(c) Relative mRNA levels of *cACTB* (β -actin) normalized by *cHPRT* in WT (blue dots) and γ -actin-KO (red dots) MDCK using RT-qPCR from 6 independent experiments. Dots shows replicates and bars represent mean \pm SD. Indicated p-values are obtained from a two-sided one-way Anova test.

(d) IF microscopy analysis and RFI quantifications of β -actin (red) at junctions in γ -actin-KO (red dots) rescued with either γ -actin (pink dots, top panels, γ -actin-KO: n=85, γ -actin-KO+ γ -actin: n=79), or GFP (green dots, bottom panels, γ -actin-KO: n=80, γ -actin-KO+GFP: n=81) from 3 independent experiments.

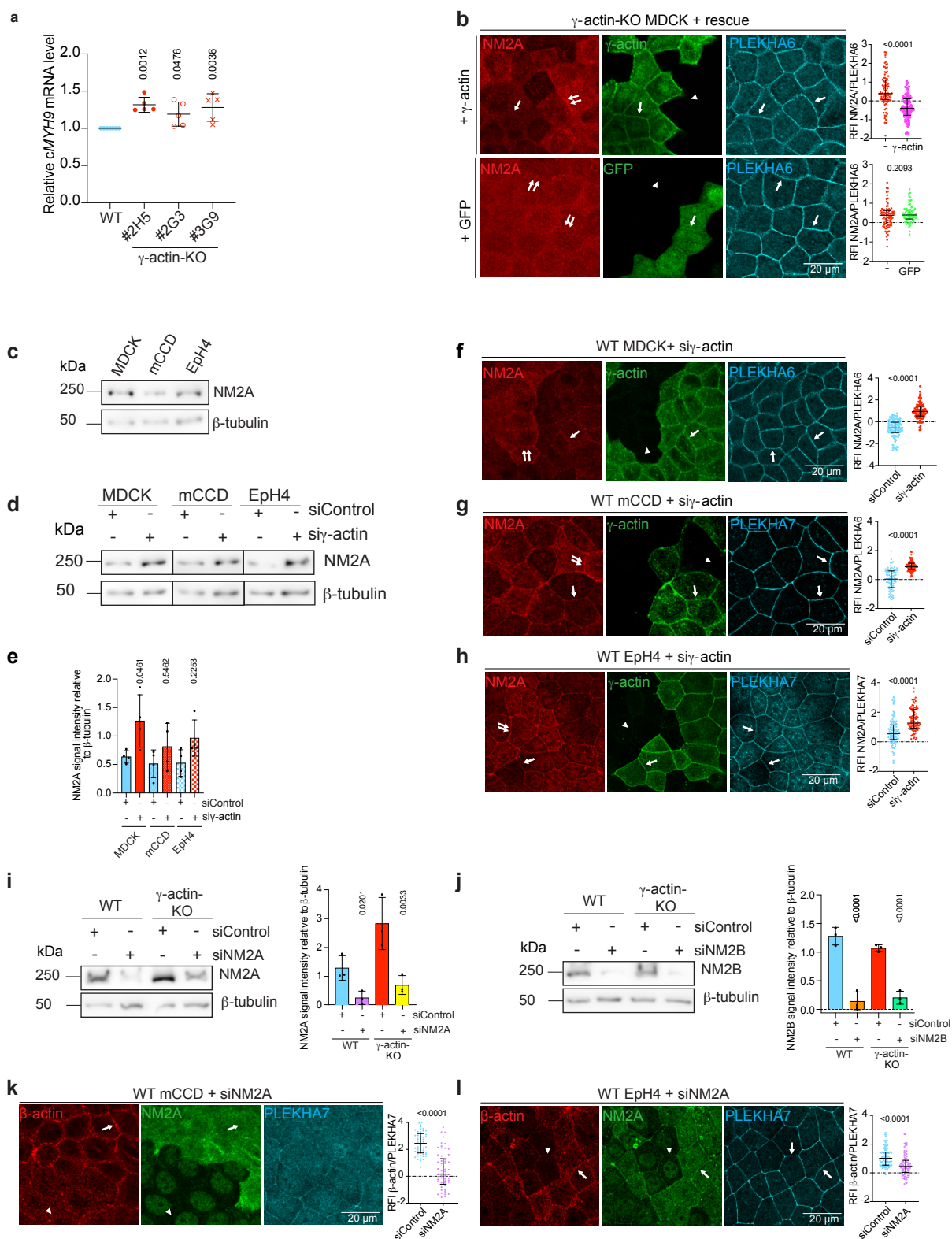
(e) IB analysis of protein level of γ -actin and GFP in lysates of WT, γ -actin-KO, and γ -actin-KO rescued with either γ -actin or GFP. 2 exposure levels were used: low and high.

(f) IB analysis of protein level of γ -actin and β -actin in lysates of WT MDCK, mCCD and EpH4 from 3 independent experiments.

(g-h) IB analysis (g) and relative densitometric quantifications (h) of protein levels of γ -actin and β -actin in lysates of WT MDCK, mCCD and EpH4 treated with siControl (blue dots) or si γ -actin (red dots) from 5 independent experiments. β -tubulin was used as a loading control. Indicated p-values are obtained from a two-sided one-way Anova test.

(i-k) IF microscopy analysis and RFI quantifications of β -actin (red) at junctions in WT (blue dots) MDCK (siControl: n=94, si γ -actin: n=100) (i), mCCD (siControl: n=132, si γ -actin: n=141) (j) or EpH4 (siControl: n=142, si γ -actin: n=137) (k) upon γ -actin depletion (red dots) from 2-3 independent experiments.

(a-b, d, i-k) KO/KD/rescue cells were distinguished from WT γ -actin or GFP (green). Arrows indicate normal labelling (as in WT). Double-arrows indicate increased labelling for β -actin. Arrowheads indicate loss of γ -actin labelling in KO or KD cells. PLEKHA6 or PLEKHA7 are used as junctional markers (cyan). Scale bar = 20 μ m. Dots shows replicates and bars represent mean \pm SD. Indicated p-values are obtained from a two-sided unpaired Mann-Whitney test. Source data for this figure are provided as a Source Data file.



Supplementary Figure 3. The KO of γ -actin specifically affects the mRNA and protein expression of NM2A in different epithelial cell types, and this in turn affects β -actin.

(a) Relative mRNA levels of *cMYH9* (NM2A) normalized by *cHPRT* in WT (blue dots) and γ -actin-KO (red dots) MDCK using RT-qPCR from 5 independent experiments. Dots shows replicates and bars represent mean \pm SD. Indicated p-values are obtained from a two-sided one-way Anova test.

(b) IF microscopy analysis and RFI quantifications of NM2A (red) at junctions in γ -actin-KO (red dots) rescued with either γ -actin (pink dots, top panels, γ -actin-KO: n=89, γ -actin-KO+ γ -actin: n=85), or GFP (green dots, bottom panels, γ -actin-KO: n=82, γ -actin-KO+GFP: n=74) from 3 independent experiments.

(c) IB analysis of protein level of NM2A in lysates of WT MDCK, mCCD and Eph4 from 3 independent experiments.

(d-e) IB analysis (d) and relative densitometric quantifications (e) of protein levels of NM2A in lysates of WT MDCK, mCCD and Eph4 treated with siControl (blue dots) or si γ -actin (red dots) from 4 independent experiments.

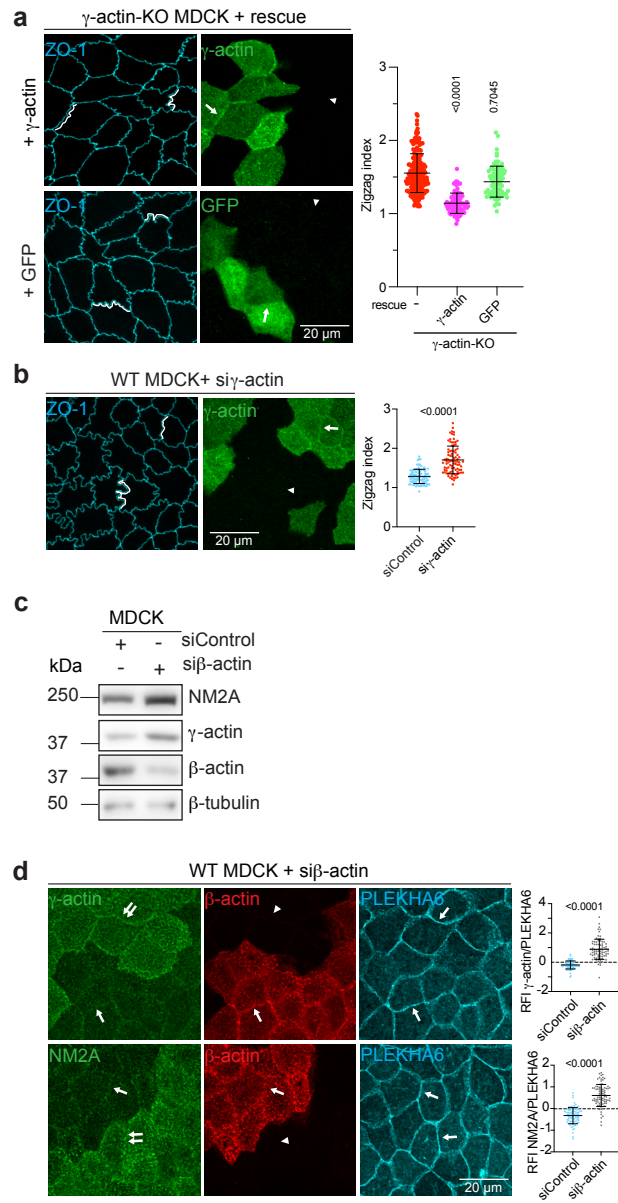
(f-h) IF microscopy analysis and RFI quantifications of NM2A (red) at junctions in WT (blue dots) MDCK (siControl: n=98, si γ -actin: n=95) (f), mCCD (siControl: n=86, si γ -actin: n=97) (g) or Eph4 (siControl: n=105, si γ -actin: n=97) (h) upon γ -actin depletion (red dots) from 2-3 independent experiments.

(i-j) IB analysis and relative densitometric quantifications of protein level of NM2A (i) or NM2B (j) in lysates of WT or γ -actin-KO treated with siControl, siNM2A or siNM2B from 3 independent experiments.

(c-e, i-j) β -tubulin was used as a loading control. Dots shows replicates and bars represent mean \pm SD. Indicated p-values are obtained from a two-sided one-way Anova test.

(k-l) IF microscopy analysis and RFI quantifications of β -actin (red) at junctions in WT (blue dots) mCCD (siControl: n=55, siNM2A: n=60) (k) or Eph4 (siControl: n=88, siNM2A: n=82) (l) upon NM2A depletion (purple dots) from 3 independent experiments.

(b, f-h, k-l) Arrows indicate normal junctional NM2A/ β -actin localization. Double-arrows indicate junctional NM2A enrichment. Arrowheads indicate decreased labelling for γ -actin/NM2A/ β -actin in KO/KD cells. PLEKHA6 or PLEKHA7 are used as junctional markers (cyan). Scale bar = 20 μ m. Dots shows replicates, bars represent mean \pm SD. Indicated p-values are obtained from a two-sided unpaired Mann-Whitney test. Source data for this figure are provided as a Source Data file.



Supplementary Figure 4. The KD of γ -actin results in increased TJ membrane tortuosity and is rescued by exogenous expression of γ -actin.

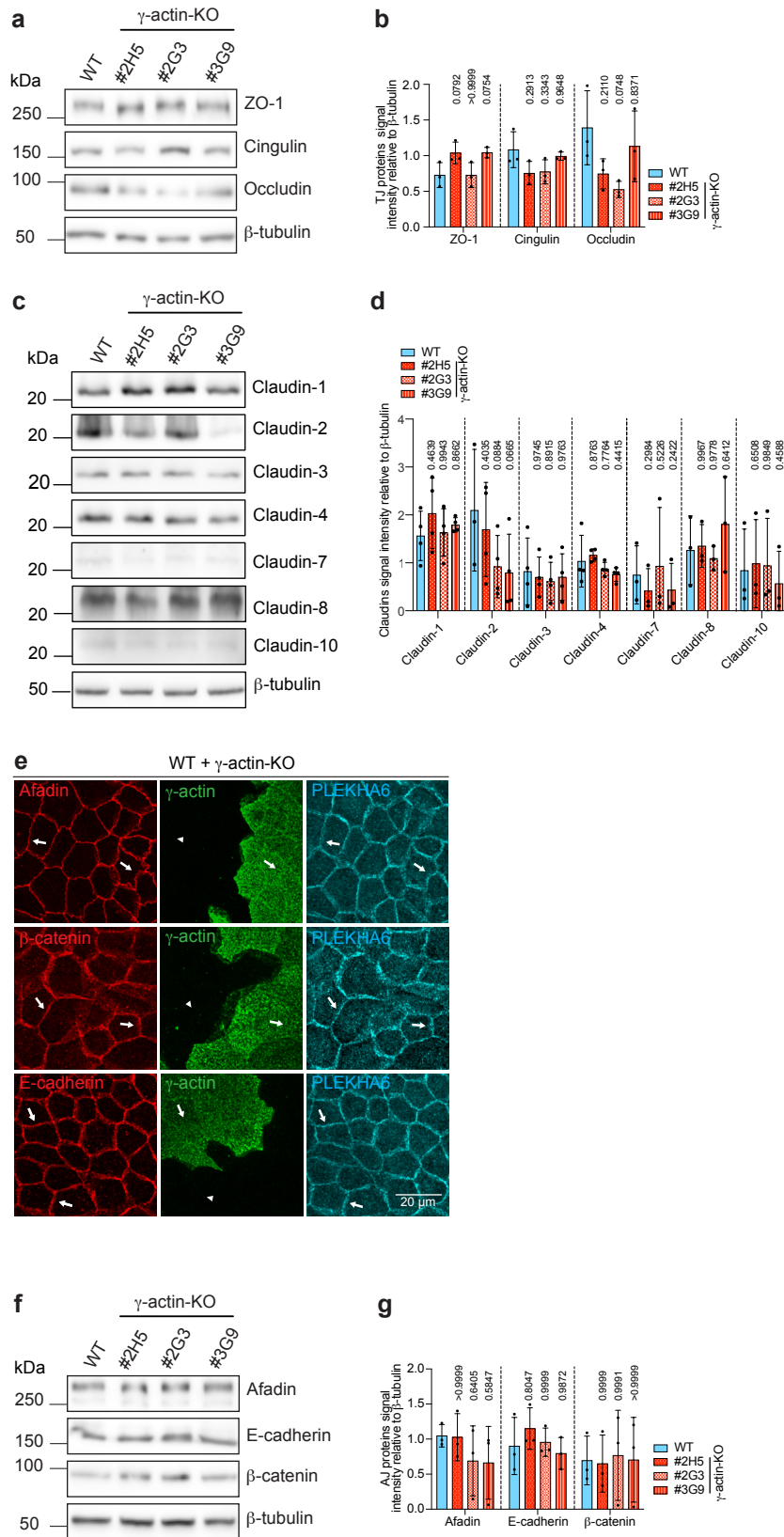
(a) IF microscopy analysis and zigzag index quantifications of ZO-1 (cyan); used as a TJ marker; in γ -actin-KO cells (red dots, n=92) rescued with either γ -actin, (pink dots, top panels, n=87), or by GFP (green dots, bottom panels, n=78) distinguished via γ -actin or GFP (green), from 3 independent experiments.

(b) IF microscopy analysis and zigzag index quantifications of ZO-1 (cyan) in WT (blue dots) MDCK cells upon γ -actin depletion (red dots) (siControl and si γ -actin: n=90), distinguished via γ -actin (green), from 3 independent experiments.

(a-b) White line represents the membrane tortuosity. Scale bar = 20 μ m. Dots shows replicates and bars represent mean \pm SD. Indicated p-values are obtained from a two-sided unpaired Mann-Whitney test.

(c) IB analysis of protein level of NM2A, γ -actin and β -actin in lysates of WT MDCK treated with siControl or si β -actin. β -tubulin was used as a loading control from 3 independent experiments. Dots shows replicates and bars represent mean \pm SD. Indicated p-values are obtained from a two-sided one-way Anova test.

(d) IF microscopy analysis and RFI quantifications of γ -actin (top panel, siControl: n=86, si β -actin: n=78) or NM2A (bottom panel, siControl: n=82, si β -actin: n=84) (green) at junctions in WT MDCK cells (blue dots) upon β -actin depletion (grey dots), distinguished via β -actin (red), from 3 independent experiments. Arrows indicate normal junctional γ -actin and NM2A localization. Double-arrows indicate junctional γ -actin and NM2A enrichment. PLEKHA6 was used as a junctional marker (cyan). Scale bar = 20 μ m. Dots shows replicates and bars represent mean \pm SD. Indicated p-values are obtained from a two-sided unpaired Mann-Whitney test. Source data for this figure are provided as a Source Data file.



Supplementary Figure 5. The KO of γ -actin does not perturb the expression of TJ, AJ and claudin proteins, and the junctional accumulation of AJ proteins in MDCK cells.

(a-d) IB analysis (a, c) and relative densitometric quantifications (b, d) of protein level of either TJ (ZO-1, cingulin and occludin, not changed) (a-b), or claudin (claudin-1, -2, -3, -4, -7, -8, -10, not changed) (c-d) proteins in lysates of WT (blue dots) and γ -actin-KO (red dots, 3 distinct clonal lines) MDCK cells from 3-4 independent experiments.

(e) IF microscopy analysis of endogenous afadin, E-cadherin and β -catenin (AJ proteins, red, not changed) in mixed cultures of WT (blue dots) and γ -actin-KO (red dots) cells, distinguished via γ -actin (green), from 2-3 independent experiments. PLEKHA6 (cyan) is used as a junctional marker. Scale bar = 20 μ m.

(f-g) IB analysis (f) and relative densitometric quantifications (g) of protein level of afadin, E-cadherin and β -catenin (not changed) in lysates of WT (blue dots) and γ -actin-KO (red dots, 3 distinct clonal lines) MDCK cells from 3 independent experiments.

(a-d, f-g) β -tubulin was used as a loading control. Dots shows replicates and bars represent mean \pm SD. Indicated p-values are obtained from a two-sided one-way Anova test. Source data for this figure are provided as a Source Data file.

Supplementary Table 1. Resources table

Reagent of resources	Source / Reference	Identifier
Antibodies		
Mouse IgG2b monoclonal anti- γ -actin (IB, IF)	Prof. C. Chaponnier, University of Geneva ¹	2A368E2 RRID:AB_2571583
Mouse IgG1 monoclonal anti- β -actin (IB, IF)	Prof. C. Chaponnier, University of Geneva ¹	4C259H12 RRID:AB_2571580
Rat polyclonal anti-PLEKHA6 (IF)	²	RtSZR127
Guinea pig polyclonal anti-PLEKHA7 (IF)	²	GP2737
Rabbit polyclonal anti-NM2A (IB, IF)	Biolegend	Cat# 909801 RRID:AB_291638
Rabbit polyclonal anti-NM2B (IB, IF)	Biolegend	Cat# 909901 RRID:AB_291639
Mouse monoclonal anti-pan-actin (IB)	Sigma-Aldrich/Merck	Cat# mab1501 RRID: AB_2223041
FITC-phalloidin (IF)	Sigma	Cat# P5282
Alexa Fluor™ 488 Phalloidin	Invitrogen™	Cat# A12379
Mouse monoclonal anti-GFP (IF)	Roche	Cat# 11814460001, RRID:AB_390913
Mouse monoclonal anti- β -tubulin (IB)	Thermo Scientific	Cat# 32-2600 RRID: AB_2533072
Rat monoclonal anti-ZO-1 (IF)	Prof. Daniel Goodenough, Harvard Medical School	R40.76, RRID:AB_2205518
Mouse monoclonal anti-ZO-1 (IB)	Thermo Scientific	Cat# 3391000 RRID: AB_2533147
Rabbit polyclonal anti-cingulin (IB, IF)	Citilab	C532
Rabbit polyclonal anti- β -catenin (IB, IF)	Sigma-Aldrich/Merck	Cat# C2206 RRID: AB_326078
Rabbit polyclonal anti-E-cadherin	Santa Cruz	Cat# 7870 RRID: AB_2076666
Mouse monoclonal anti-E-cadherin	BD Biosciences	Cat# BD 610181 RRID:AB_397580
Rabbit polyclonal anti-Claudin-1 (IB)	Thermo Scientific	Cat# 51-9000 RRID: AB_2533916
Mouse monoclonal anti-Claudin-2 (IB)	Thermo Scientific	Cat# 32-5600 RRID: AB_2533085
Rabbit polyclonal anti-Claudin-3 (IB)	Thermo Scientific	Cat# 34-1700 RRID: AB_2533158
Mouse monoclonal anti-Claudin-4 (IB)	Thermo Scientific	Cat# 32-9400

		RRID: AB_2533096
Rabbit polyclonal anti-Claudin-7 (IB)	Thermo Scientific	Cat# 34-9100 RRID: AB_2533190
Rabbit polyclonal anti-Claudin-8 (IB)	Thermo Scientific	Cat# 40-0700Z RRID: AB_2533445
Rabbit polyclonal anti-Claudin-10 (IB)	Thermo Scientific	Cat# 38-8400 RRID: AB_2533386
Cy3-AffiniPure Donkey anti-Mouse IgG	Jackson Laboratory	Cat# 715-165-151 RRID: AB_2315777
Cy3-AffiniPure Donkey anti-Rat IgG	Jackson Laboratory	Cat# 712-166-150 RRID: AB_2340668
Alexa Fluor 488-AffiniPure Donkey anti-Rabbit IgG	Jackson Laboratory	Cat# 711-545-152 RRID: AB_2313584
Cy5-AffiniPure Donkey anti-Rat IgG	Jackson Laboratory	Cat# 712-175-153 RRID: AB_2340672
Cy5-AffiniPure Donkey anti-Mouse IgG	Jackson Laboratory	Cat# 715-175-150 RRID: AB_2340819
Anti-mouse IgG (H+L), HRP Conjugate	Promega	Cat# W4021 RRID: AB_430834
Anti-rabbit IgG (H+L), HRP Conjugate	Promega	Cat# W4011 RRID: AB_430833
Plasmids		
pTRE2Hyg-GFP-myc	3	S1210
pTRE2Hyg-GFP-cingulin-FL-myc	4	S1052
pTRE2Hyg-GFP-ZO-1-FL	5	S2474
pTRE2Hyg-ACTG1-FL	This paper	S2882
pTRE2Hyg-ACTB-FL	This paper	S2926
Chemicals, Reagents, Peptides, Critical commercial assays		
Pierce Protease Inhibitor Tablet, EDTA-free	Thermo Scientific	Cat# A32965
jetOPTIMUS	Polyplus	Cat# 117-15
Lipofectamine RNAiMAX	Invitrogen	Cat# 13778030
Hanks buffer	Gibco	Cat# 14025-050
3 kDa fluorescein-dextran	Invitrogen	Cat# D3305
OptiMeM	Gibco	Cat# 51985-026
DMEM without phenol red	Gibco	Cat# 21063-029
NucleoSpin® RNA kit	Macherey-Nagel	Cat# 740955.50
iScript™ cDNA Synthesis kit	Bio-Rad	Cat# 1708890
Master Mix Select SYBR™ kit	Thermo Scientific	Cat# 4472908
Pierce BCA Protein assay kit	Thermo Scientific	Cat# 23225

WesternBright ECL kit	Advansta	Cat# K-12045-D50
Molecular Weight Markers for SDS-PAGE	BioRad	Cat# 1610373
DNeasy Blood and Tissue kit	Qiagen	Cat# 69504
Hoechst	Thermo Scientific	Cat# 33342
Blebbistatin	Sigma-Aldrich/Merck	Cat# B0560
Bovines Serumalbumin (BSA)	Carl Roth GmbH	Cat# 3737.1
Dulbecco's Phosphate Buffered Saline (PBS)	Gibco™	Cat# 21600-051
Glass coverslips 1.5H 22 x 22 mm	Carl Roth GmbH	Cat# KCY1.1
Microscope slides, corners grounded 90°, without frosted edge	Carl Roth GmbH	Cat# H869.1
Mowiol® 4-88	Carl Roth GmbH	Cat# 0713.2
Paraformaldehyde (PFA)	Science Services	Cat# E15714
Poly-D-Lysine Hydrobromide	Sigma-Aldrich	Cat# P7405-5MG
6-well tissue culture plate, flat bottom, polystyrene	TPP Techno Plastic Products AG	Cat# 92406
Experimental models: Cell lines		
Madin-Darby Canine Kidney Tet-Off (MDCK) WT	A. Fanning, University of North Carolina	Clontech
Madin-Darby Canine Kidney Tet-Off (MDCK) γ -actin-KO	This paper	N/A
Mouse mammary epithelial cell line (Eph4) WT	Reichmann Laboratory, ⁶	N/A
Mouse Cortical Collecting Duct Cell Line (mCCD) WT	Férraille Laboratory, University of Geneva ⁷	N/A
Oligonucleotides		
siRNA targeting sequence : canis γ -actin GUUAACUGUCCCUUGGUAUA	This paper	Microsynth
siRNA targeting sequence : canis β -actin AAACCUAACUUGCGCAGAA	This paper	Microsynth
siRNA targeting sequence : canis NM2A GAAGAUCACAGACGUCAUUAU	This paper	Microsynth
siRNA targeting sequence : canis NM2B GCUACUAUUCGGGAUUGAUCU	This paper	Microsynth
siRNA negative control: CGUACGCGGAUACUUCGA	This paper	Microsynth
CRISPR target sequence: canis <i>ACTG1</i> TCTACGAGGGGTACGCCTTG	This paper	Genscript
CRISPR target sequence: canis <i>ACTG1</i> GAAGCTCTGCTACGTCGCCC	This paper	Genscript

RT-qPCR target sequence: canis <i>ACTB</i> Fw: AGCGCAAGTACTCTGTGTGG Rv: GTAACAGTCCGCCTAGAAGC	This paper	Microsynth
RT-qPCR target sequence: canis <i>MYH9</i> Fw: CTGCAAAGTGGCCAAGGAGA Rv: GTCGGTGATCATCGCCTCAT	This paper	Microsynth
RT-qPCR target sequence: canis <i>HPRT</i> Fw: TGGACAGGACTGAGCGGC Rv: TGAGCACACAGAGGGCTACG	This paper	Microsynth
Software and algorithms		
Image J	N/A	Imagej.nih.gov/ij/ RRID: SCR_003070
Affinity Designer	N/A	https://affinity.serif.com/ RRID: SCR_016952
Prism GraphPad	N/A	https://www.graphpad.com/scientific-software/prism/ RRID: SCR_002798
Snapgene Version 3.1.2	N/A	snapgene.com RRID:SCR_015052

References for Supplementary Table 1

1. Dugina V, Zwaenepoel I, Gabbiani G, Clement S, Chaponnier C. Beta and gamma-cytoplasmic actins display distinct distribution and functional diversity. *J Cell Sci* **122**, 2980-2988 (2009).
2. Sluysmans S, *et al.* PLEKHA5, PLEKHA6 and PLEKHA7 bind to PDZD11 to target the Menkes ATPase ATP7A to the cell periphery and regulate copper homeostasis. *Mol Biol Cell* **32**, 1-20 (2021).
3. Zheng CY, Petralia RS, Wang YX, Kachar B. Fluorescence recovery after photobleaching (FRAP) of fluorescence tagged proteins in dendritic spines of cultured hippocampal neurons. *J Vis Exp*, (2011).
4. D'Atri F, Citi S. Cingulin interacts with F-actin in vitro. *FEBS Lett* **507**, 21-24 (2001).
5. Mauperin M, Sassi A, Mean I, Feraille E, Citi S. Knock Out of CGN and CGNL1 in MDCK Cells Affects Claudin-2 but Has a Minor Impact on Tight Junction Barrier Function. *Cells* **12**, (2023).
6. Fialka I, Schwarz H, Reichmann E, Oft M, Busslinger M, Beug H. The estrogen-dependent c-JunER protein causes a reversible loss of mammary epithelial cell polarity involving a destabilization of adherens junctions. *J Cell Biol* **132**, 1115-1132 (1996).
7. Wang YB, *et al.* Sodium transport is modulated by p38 kinase-dependent cross-talk between ENaC and Na,K-ATPase in collecting duct principal cells. *J Am Soc Nephrol* **25**, 250-259 (2014).

Supplementary notes

Abbreviations

AJC, apical junctional complex; KO, knock-out; FRAP, fluorescence recovery after photobleaching; TJ, tight junction; AJ, adherens junction; NM2, non-muscle myosin-2; KD, knock-down; IB, immunoblot; IF, immunofluorescence; pMLC2, phosphorylated myosin light chain 2; TER, transepithelial resistance; AFM, atomic force microscopy; FSC-A, forward scatter area; MLCK, myosin light chain kinase; ABR, actin binding region; Madin-Darby Canine Kidney-II, MDCK; mCCD, mouse cortical collecting duct; EpH4, mouse mammary; DMEM, Dulbecco's Modified Eagle's; FBS, Fetal Bovine Serum; NEAA, non-essential amino-acids; P/S, penicillin and streptomycin; gRNA, guide RNA; GFP, green fluorescent protein; RT, room temperature; NaCl, sodium chloride; RIPA, radioimmunoprecipitation assay buffer; EDTA, ethylenediaminetetraacetic acid; SDS, sodium dodecyl sulfate; O₂, oxygen; CO₂, carbon dioxide; FC, fold change; FDR, false discovery rate; PIC, protease inhibitor cocktail; PFA, paraformaldehyde; BSA, bovine serum albumin; DAPI, 4',6 diamidino 2 phenylindole; FL, full-length; HBSS, Hank's balanced salt solution; GLM, general linear model; hr, hour; s, seconds; Perm_{app}, apparent permeability; PBS, phosphate buffered saline; DPBS, Dulbecco's phosphate buffered saline; S-MEM, suspension-minimum essential medium; EGF, epidermal growth factor; PLEKHA6, Pleckstrin Homology Domain-Containing, family A member 6; kDa, kilodaltons; ECL, enhanced chemiluminescence; SD, standard deviation; Px, pixels; RFI, relative fluorescence intensity; ns, not significant; WT, wild-type.